主論文

Petrology of Pelitic Schists in the Oligoclase-Biotite Zone of the Sanbagawa Metamorphic Terrain, Japan; Phase Equilibria in High-Grade Zone of an Intermediate High-Pressure Metamorphism

三波川変成帯の灰曹長石ー黒雲母帯における泥質片岩の岩石学的研究：
とくに高圧中間群変成作用の高温部における相平衡の解析

Journal of Metamorphic Geology
Vol. 1 (1983, in press)

榎並正樹

Petrology of Pelitic Schists in the Oligoclase-Biotite Zone of the Sanbagawa Metamorphic Terrain, Japan; Phase Equilibria in High-Grade Zone of an Intermediate High-Pressure Metamorphism

Masaki Enami

Department of Earth Sciences, Nagoya University, Nagoya 464, Japan

Running Title: Oligoclase-Biotite Zone of the Sanbagawa Metamorphic Terrain

Jour. Meta. Geol. (1983 in press)

Abstract. The oligoclase-biotite zone of the Bessi area, central Shikoku is characterized by sodic plagioclase (X_{Ca} = Ca/(Ca + Na) = 0.10-0.28)-bearing assemblages in pelitic schists, and represents the highest-grade zone of the Sanbagawa metamorphic terrain. Mineral assemblages of pelitic schists in this zone, all with quartz, sodic plagioclase, muscovite and clinozoisite (or zoisite), are garnet + biotite + chlorite + paragonite, garnet + biotite + hornblende + chlorite, and partial assemblages of the above types. Correlations between mineral compositions, mineral assemblages and mineral stability data assuming $P_{H_2O} = P_{solid}$ suggest that metamorphic conditions of this zone are about 610 ± 25 °C and 10 ± 1 Kb.

Based upon the comparative study of mineralogy and chemistry of pelitic schists in the oligoclase-biotite zone with those in New Caledonia omphacite zone as a typical high-pressure type and with those in upper staurolite zone as a medium-pressure type, progressive assemblages within these three zones can be related by such reactions as:

<u>omphacite zone</u>

garnet + glaucophane + omphacite + muscovite =

<u>oligoclase-biotite zone</u>

biotite + hornblende + plagioclase + quartz + H_2O

oligoclase-biotite zone

garnet + hornblende + paragonite + muscovite =

upper staurolite zone

staurolite + biotite + plagioclase + quartz + H_2O

dP/dT values of these equations calculated using natural compositions are 3-6 and 16-19, respectively, and their gradients are gentle. This implies that the contrasts of mineral parageneses in pelitic schists related by the above equations result mainly from the difference in pressure during progressive metamorphism. A combination of mineral assemblages observed in the Sanbagawa oligoclase-biotite zone represents a characteristic mineral paragenesis of pelitic schists in the high-grade part of an intermediate high-pressure metamorphism.

Introduction

The Sanbagawa metamorphic terrain is a typical intermediate high-pressure metamorphic terrain introduced by Miyashiro (1961), which extends from the Kanto Mountains, northwest of Tokyo, through Shikoku (island), to eastern Kyushu for about 800 km with a maximum width of 40 km in central Shikoku. Detailed zonal mappings of the Sanbagawa terrain have been well performed in central Shikoku and their compilation is available in Banno et al.

(1978). On the basis of mineral paragenesis in pelitic schists*, Higashino (1975) and Banno et al. (1978) divided the Sanbagawa terrain in central Shikoku into chlorite, garnet and biotite zones, in the ascending order of metamorphic grade. Recently, Enami (1981, 1982) reported that some of plagioclases in the high-grade part of the biotite zone in the Bessi area are calcic, X_{Ca} = 0.28 in maximum and commonly X_{Ca} = 0.15-0.20**. The biotite zone can be divided into two subzones on the basis of compositional variations of plagioclase coexisting with clinozoisite (or zoisite) and quartz in pelitic schists and additionally in epidote amphibolites: the lower-grade albite-biotite zone and the higher-grade oligoclase-biotite zone.

X_{Ca} of plagioclase coexisting with epidote group minerals increases, in general, with increasing metamorphic grade. In high-pressure regional metamorphic terrains, however, plagioclase has albitic compositions, and oligoclase or more calcic plagioclase have not been confirmed, except for a few data. Plagioclase with X_{Ca} = 0.1-0.4 was reported from the Lepontine Alps (e.g., Ernst 1973, 1977), but was formed by a medium-pressure metamorphism superposed on the Early Alpine metamorphism of high-pressure. Calcic plagioclase, which is now completely saussuritized, was described by Platt (1975) from amphibolite tectonic slices in St. Catalina island of the Franciscan terrain, but

it is not certain whether or not these tectonic slices constitute really a progressively high-grade equivalent of the Franciscan metamorphic rocks (Coleman and Lanphere 1971). Therefore, the Bessi area is said to be the only high-pressure metamorphic terrain where sodic plagioclase, not albite, occurs in the higher-grade zone of a progressive metamorphism.

In this paper, the author will discuss the paragenetic relation of pelitic schists in the oligoclase-biotite zone, in order to decipher the nature of the high-grade part of a high-pressure metamorphism. The mineral paragenesis is also comparatively discussed between the Sanbagawa oligoclase-biotite zone and some other medium- or high-pressure metamorphic terrains.

Outline of geology and petrography

Figure 1 shows a geological map of central Shikoku with the location of the Bessi area. The Bessi area is located to the northwest of the Shirataki area (Ernst et al. 1970) and covers the higher-grade portion of the Bessi-Ino district investigated by Banno (1964). This area is underlain by the Minawa and Ojoin formations as defined by Kojima and his coworkers (e.g., Kojima et al. 1956).

Large peridotite (Higashi-akaishi mass)-epidote amphibolite (Tonaru and Iratsu masses) complex occurs in the upper member of

the Minawa formation, which is composed mainly of interbedded basic and pelitic schists. The Tonaru and Iratsu masses are metamorphosed layered gabbros (Banno et al. 1976; Yokoyama 1980; Takasu and Makino 1980), and have been subjected to the Sanbagawa progressive metamorphism up to the epidote amphibolite facies with the surrounding crystalline schists and peridotite (Mori and Banno 1973, Yokoyama 1980; Kunugiza 1980; Enami 1982).

Figure 2 shows a metamorphic zonation map of the Bessi area with the localities of samples discussed in detail. A schematic stability relationship of minerals in pelitic schists in regard to the metamorphic grade is given in Fig. 3. The garnet zone is defined by the presence of pyralspite garnet which usually contains 3-5 wt% of MnO at the rim and by the absence of biotite in pelitic schists, and is not, strictly speaking, an almandine zone. Owing to the presence of peristerite solvus, X_{Ca} value of plagioclase increases discontinuously from about 0.05 to 0.10 with increasing metamorphic grade at the boundary between the albite- and oligoclase-biotite zones. In the oligoclase-biotite zone, chlorite is a minor constituent and pelitic schists have usually garnet + biotite + hornblende assemblage showing a contrast with a common assemblage of garnet + biotite + chlorite in the albite-biotite zone.

The oligoclase-biotite zone includes epidote amphibolites and the

surrounding schists, and its regional distribution roughly corresponds to the Zone E of Banno's (1964) zonal mapping. This zone extends from the western margin of the Tonaru mass eastwards to the western part of the Iratsu mass for about 9 km with a width of 1-3 km. The eastern border of the zone is situated within the Iratsu mass and does cut the lithologic boundary between epidote amphibolites and schists. The regional distribution of the oligoclase-biotite zone is consistent with the regional thermal structure of the Sanbagawa terrain in central Shikoku proposed by Banno et al. (1978). Not any significant break in geological structure and metamorphic grade has been observed around the oligoclase-appearance line.

In the Bessi area, schists occur trending E-W with a northerly dip, as if the structure is monoclinal, but the highest metamorphic grade zone lies in middle of the apparent stratigraphy, from which the metamorphic grade decreases both up- and down-wards. This thermal structure was interpreted to have resulted from a large-scale recumbent fold postdated the Sanbagawa progressive metamorphism (Banno et al. 1978).

Mode of occurrence and chemistry of minerals

Table 1 lists the mineral assemblages of pelitic schists in the oligoclase-biotite zone examined in detail. The localities of the

samples referred to herein are shown in Fig. 2.

Detailed mineralogical works were done with an electron-probe microanalyzer, JXA-5A of JEOL. Except for plagioclase, the observed intensities for minerals were corrected by the method of Bence and Albee (1968). Plagioclase was analyzed by the partial analytical method proposed by Yusa (1975). Accelerating voltage, specimen current and beam diameter were kept at 15 kv, 0.010-0.012 μA and 3-5 μm, respectively. Table 2 lists representative chemical compositions of major constituent minerals. A table of analyses of other samples described in this papaer is available upon request.

Plagioclase

Plagioclase occurs usually as porphyroblasts measuring about 1-5 mm in size and sometimes exhibits myrmekitic texture defined by randomly orientated quartz vermicles in plagioclase. It occurs also as mosaic aggregates of plagioclase and quartz crystals, or else, of plagioclase alone. These plagioclases are commonly zoned and X_{Ca} values are usually 0.13-0.15 in the core and 0.20-0.25 in the rim. K_2O content is less than 0.1 wt%.

In some samples, coexistence of oligoclase and albite is observed in two modes of occurrence: (1) coexistence as discrete grains and (2) composite grains consisting of albite core and discontinuous

oligoclase rim (Enami 1981, 1982). Coexisting two plagioclases of the former type occur only in samples collected from the low-grade part of the oligoclase-biotite zone. This type of albite-oligoclase pair indicates the presence of peristerite solvus in this grade, and will be discussed elsewhere (Enami in prep.). Coexisting two plagioclases of the latter type occur throughout the oligoclase-biotite zone. In some samples having composite grains, discrete oligoclase crystals also occur having the same composition with the oligoclase rim of the composite grains, but albite was always enclosed by oligoclase. These chemical and textural relations suggest that, as well as the discrete crystals, the oligoclase rim of the composite grains was in equilibrium with other constituents, but the albite core is a relict crystal formed at an early stage of the Sanbagawa progressive metamorphism. In the samples examined in detail two plagioclases, when present, form the composite grains, and outermost rim composition having a maximum X_{Ca} was chosen for the discussion of mineral paragenesis.

Garnet

Garnet is usually euhedral but sometimes shows subhedral form, being replaced by biotite and/or chlorite. In the euhedral garnet, distinct two types of zonal structure were observed. Garnet shows

usually a normal type of zonal structure in which X_{Mg} value (= Mg/(Mg + Fe)) increases and Mn content decreases from the core towards the rim. In the other type of zoned garnet, Mn content has a minimum at an intermediate part of the zonal structure and X_{Mg} values increases monotonously from the core to the rim.

In both two types of zoned garnet, Ca content has a maximum in an intermediate part of the zonal structure like high-grade samples from the other Sanbagawa terrain (cf. Banno and Kurata 1972; Enami 1982).

In the rim, it is Ca-rich almandine (X_{Mg} = 0.15 ± 0.04 and X_{Ca} (= Ca/(Ca + Fe + Mg + Mn)) = 0.26 ± 0.03) with 1.2 ± 0.5 wt% of MnO, and more enriched in pyrope and grossular components than that in the albite-biotite zone (X_{Mg} = 0.11 ± 0.02 and X_{Ca} = 0.23 ± 0.03, Kurata and Banno 1974; Higashino 1975).

Biotite

Biotite has brownish varieties and occurs in three modes of occurrence: (1) replacing garnet or formed in its pressure shadow, (2) dispersed in the matrix with nematoblastic texture and (3) inclusion in prograde minerals such as garnet and plagioclase. Compositional relation of biotite of the three modes is shown in Fig. 4.

The matrix and inclusion biotites have a chemical composition similar to each other, but tend to be more enriched in Mg than the

pseudomorphous biotite after garnet. The biotite replacing garnet postdated the formation of garnet porphyroblast, and hence the matrix and inclusion biotites with higher X_{Mg} value are regarded as a product in the Sanbagawa progressive metamorphism.

TiO_2 content of the primary biotite is 1.6 ± 0.2 wt% similar to that in the albite-biotite zone, while X_{Mg} value is about 0.59 ± 0.06 and higher (TiO_2 = 1.6 ± 0.3 wt% and X_{Mg} = 0.47 ± 0.04 in the albite-biotite zone, Kurata and Banno 1974; Higashino 1975).

Hornblende

Hornblende is a common constituent mineral and has pale green or bluish green Z-axial color. It is usually homogeneous, but two types of zonal structure, with regard to Al content, were distinctly observed in some grains (cf. Enami 1982). In most zoned hornblendes, Al contant increases from the core towards the rim, with the interval of about 4 wt% of Al_2O_3 at maximum. Reverse-zoned hornblende, which consists of homogeneous and Al-rich core and less aluminous rim, was also observed. The Al-poor rim of the reverse-zoned hornblende is usually actinolitic (Al_2O_3 = 1-8 wt%). As well as the homogeneous hornblende, the Al-richer portion of the zoned crystal is regarded as a prograde product on the following reasons. Firstly, increase in Al content of calcic amphiboles

with increasing grade has been recognized in many low- to medium-grade metamorphic terrains, and is also valid in the Sanbagawa metamorphic terrain (Banno 1964; Ernst et al. 1970; Otsuki and Banno in prep.). Secondly, composition of the Al-rich portion is usually the same for grains in a thin section, even if the zoning patter is different for each grain. It is also similar to the composition of the coexisting homogeneous hornblende. Thirdly, reverse-zoned hornblende was hardly observed in inclusions of prograde minerals, though it occurs usually in the matrix (Enami 1982).

The primary hornblende has X_{Mg} value (0.59 ± 0.04) higher than that in the albite-biotite zone (X_{Mg} = 0.52 ± 0.04, Ernst et al. 1970; Higashino et al. 1981), but Al content is similar to each other (Al_2O_3 = 15.7 ± 0.7 wt% for the oligoclase biotite zone and 15.0 ± 0.9 wt% for the albite-biotite zone).

Chlorite

Chlorite is a minor constituent (modal composition is usually less than 1 %) and is absent in some samples. It, when presents, occurs in two petrographycally distinct associations: (1) chlorite forms a liniation and (2) that occurs as a pseudomorph after garnet. Type (1) chlorite itself is sometimes heterogeneous consisting of high and low X_{Mg} domains. As pointed out by Kurata (1972),

the chemistry of the low X_{Mg} domain of the type (1) chlorite and that of the type (2) one is similar to each other (X_{Mg} = 0.57 ± 0.04 and MnO = 0.21 ± 0.04 wt%), while the high X_{Mg} domain has distinctly different composition (X_{Mg} = 0.64 ± 0.03 and MnO = 0.11 ± 0.06). The type (2) chlorite clearly postdated the formation of garnet, and hence the high X_{Mg} domain of the type (1) chlorite is considered to be a prograde product.

The primary chlorite is pale greenish in color and gray or brownish gray in interference color. Its X_{Mg} value is higher than that in the albite-biotite zone (X_{Mg} = 0.53 ± 0.05, Kurata and Banno 1974; Higashino 1975).

Muscovite and paragonite

Both muscovite and paragonite occur in coarse-grained (0.1-1.0 mm in size) and prismatic formes. Muscovite is enriched in FeO (1.7 ± 0.3 wt%) and MgO (2.2 ± 0.4 wt%). Celadonite content of muscovite, being measured in terms of X_{Si} = (Si/2)-3 (for O = 22), varies from 0.18 to 0.33. Paragonite is poor in FeO (0.27 ± 0.08 wt%), MgO (0.11 ± 0.05 wt%) and CaO (0.09 ± 0.04 wt%), and shows minor celadonite solid solution (X_{Si} is less than 0.05).

Figure 5 shows a relationship between X_{Na} (= Na/(Na + K)) and X_{Si} of coexisting muscovite and paragonite. In this figure, data other than for pelitic schists of the oligoclase-biotite zone were

also plotted for comparison. X_{Na} of muscovite decreases with increasing X_{Si}, and increases with increasing metamorphic grade for the fixed X_{Si}. Extrapolating the negative correlation between the X_{Na} and X_{Si} values to $X_{Si} = 0$ (Si = 6 for O = 22), the author estimates X_{Na} of muscovite coexisting with paragonite to be about 0.30 for the oligoclase-biotite zone samples in the celadonite-free system. X_{Na} of paragonite in muscovite-bearing samples is about 0.91 in the oligoclase-biotite zone. It follows that under the oligoclase-biotite zone conditions a compositional gap in the celadonite-free muscovite-paragonite system lies between X_{Na} = 0.30 and 0.91. Muscovite in paragonite-free samples is more depleted in Na ($X_{Na} = 0.14 \pm 0.03$ and $X_{Si} = 0.24 \pm 0.05$) than that coexsiting with paragonite, as is expected from the solvus.

Clinozoisite and zoisite

Clinozoisite and zoisite occur as common epidote group minerals in pelitic schists. There are two types of zonal structure: one with X_{Fe}^{3+} (= $Fe^{3+}/(Fe^{3+} + Al)$ assuming all Fe is Fe^{3+}) increasing from the core towards the rim, and the other with X_{Fe}^{3+} decreasing from the core towards the rim. The former type of zonal structure was observed in both clinozoisite and zoisite, but the latter only in clinozoisite. X_{Fe}^{3+} variations between the core and the rim are 0.05 for clinozoisite and 0.01 for zoisite at maximum, and average X_{Fe}^{3+} values are 0.14 and 0.04, respectively.

Discussion

Mineral paragenesis

In the oligoclase-biotite zone, the mineral assemblage of pelitic schists can be classified into the following six types: garnet + biotite + chlorite + paragonite, garnet + biotite + hornblende + chlorite, garnet + biotite + chlorite, garnet + biotite + hornblende, garnet + hornblende + chlorite, and garnet + biotite. All these minerals coexist with quartz, sodic plagioclase, muscovite and clinozoisite (or zoisite).

The stability relations of these minerals have to be discussed in terms of the system of SiO_2-Al_2O_3-Fe_2O_3-FeO-MgO-CaO-Na_2O-K_2O-H_2O with excess of quartz, sodic plagioclase, muscovite and H_2O-predominant fluid, and thus can be effectively treated in terms of the system of Al_2O_3-Fe_2O_3-FeO-MgO-CaO. Many authors have shown that Fe_2O_3 is sometimes contained as a major component in some mafic minerals especially of basic rocks, and affects the stabilities of them. Fe^{3+}/Fe^{2+} values of mafic minerals in pelitic schists containing pyrrhotite and/or graphite, however, are extremely lower than those in basic rocks (about 0.07, 0.12 and 0.05 for biotite, hornblende and chlorite, respectively, Banno 1964), and clinozoisite is the only Fe^{3+}-predominant phase in pelitic schists. In this paper, Fe_2O_3 is assumed to be fixed only in clinozoisite and hardly affects the phase relation in pelitic schists. Consequently,

the mineral paragenesis of pelitic schists can be discussed in the four components system of Al_2O_3-FeO-MgO-CaO.

Figure 6 shows critical chemical features of mafic minerals to discuss the paragenetic relation between pelitic schists.

Two divariant assemblages were observed in pelitic schists of the oligoclase-biotite zone: one is garnet + biotite + chlorite + paragonite and the other is garnet + biotite + hornblende + chlorite.

As clearly shown in Fig. 6a, garnet, biotite and chlorite in the former assemblage have X_{Mg} value lower than that of the latter one, respectively. The garnet + biotite + chlorite + paragonite assemblage represents the lowest X_{Mg} paragenesis among the chlorite-bearing ones. It is also worthy to mention that garnet in hornblende-bearing samples is more enriched in CaO than that in hornblende-free ones for the fixed X_{Mg} value (Fig. 6b).

This suggests that hornblende-bearing samples represent more Ca-enriched bulk composition than do hornblende-free ones.

On the basis of these available data, mineral paragenesis in pelitic schists of the oligoclase-biotite zone can be schematically illustrated in A (Al-1.5Na-3K)-F (Fe^{2+})-M (Mg)-C (Ca-0.25Na) tetrahedron (Fig. 7), on the assumption that X_{Ca} of sodic plagioclase is 0.2.

The phase relation shown in Fig. 7 was mainly based upon the mineralogical data of four phases divariant assemblages, and those of three phases assemblages are also consistent with what expected

from this figure (cf. Fig. 6a): (1) garnet + biotite + chlorite assemblage has intermediate X_{Mg} values between the two divariant assemblages and (2) garnet + hornblende + chlorite assemblage has X_{Mg} values higher than the garnet + biotite + hornblende + chlorite one*.

Not all the mineral assemblages projected in Fig. 7 are confirmed in pelitic schists of the oligoclase-biotite zone, but some of them were observed in pelitic schists of the albite-biotite zone and in other rock-types (see Fig. 6a and appendix). We may fully use the mineralogical data of these samples to check the adequacy of paragenetic relations proposed.

Three phases assemblage of biotite + hornblende + chlorite was confirmed in a basic schist of the oligoclase-biotite zone (sample OB-01). This sample contains no graphite but pyrrhotite, and the $X_{Fe^{3+}}$ value of clinozoisite is about 0.14. X_{Mg} values of biotite, hornblende and chlorite are 0.73, 0.67 and 0.68, respectively, and higher than those of pelitic schists with garnet + biotite + hornblende + chlorite assemblage, as is expected from Fig. 7.

Four phases assemblage of garnet + hornblende + chlorite + paragonite was confirmed in an epidote amphibolite collected from the Iratsu mass belonging to the albite-biotite zone (sample AE-01). X_{Mg} values of garnet, hornblende and chlorite in this sample are 0.25, 0.67 and 0.70, respectively, and higher than those of pelitic schists with garnet + hornblende + chlorite assemblage in the

oligoclase-biotite zone. The epidote amphibolite sample was equilibrated under slightly lower-grade conditions than the pelitic schists in the oligoclase-biotite zone, and hence we could not compare quantitatively its mineral chemistry with those in the oligoclase-biotie zone. However, if we consider the fact that in the Sanbagawa metamorphic terrain X_{Mg} values of garnet and hornblende coexisting with chlorite increase with increasing metamorphic grade (e.g., Higashino 1975; this study), the high X_{Mg} values of the Iratsu sample do not contradict what expected from the paragenetic relationship shown in Fig. 7. This assemblage may limit the highest X_{Mg} bulk composition of rocks in which garnet is stable.

Microcline + garnet assemblage was observed in a pelitic schist from the albite-biotite zone (sample AP-01). In this sample, garnet has a X_{Mg} value ($X_{Mg} = 0.02$) extremely lower than that in microcline-free pelitic schists of the same zone ($X_{Mg} = 0.11 \pm 0.02$). As pointed out by Guidotti (1974), this assemblage represents a low X_{Mg} and Al-poor bulk composition.

In conclusion, mineralogical data other than those of pelitic schists in the oligoclase-biotite zone do not contradict what expected from Fig. 7, and the paragenetic relationship proposed is regarded as that in the oligoclase-biotite zone.

Figure 7 gives also some information for the stability of staurolite in the Sanbagawa terrain. Staurolite composition is plotted in this

figure, on the Al-rich and/or Ca-rich side of the garnet-hornblende-paragonite plane. This suggests that staurolite can not coexist with both biotite and chlorite, which are common constituents of the Sanbagawa pelitic schists in the oligoclase-biotite zone (also cf. Figs. 11b and c). This feature shows a distinct contrast to a common occurrence of staurolite + biotite assemblage in pelitic schists of the medium-pressure metamorphic terrains. It follows that staurolite in the oligoclase-biotite zone occurs only in rocks which are Ca- and Al-richer and probably have lower X_{Mg} value than the ordinary Sanbagawa pelitic schists, even if staurolite is stable in this grade. This could explain why staurolite is common in medium-pressure terrains but is apparently absent in the Sanbagawa oligoclase-biotite zone. Suitable bulk composition of rocks for staurolite-bearing assemblages may be expected in FeO-enriched parts of epidote amphibolites in the Tonaru and Iratsu masses.

Physical conditions during the metamorphism

As discussed by Yokoyama (1980) and Brothers and Yokoyama (1982), the critical criterion that difines the temperature-pressure conditions during the metamorphism of the oligoclase-biotite zone is based upon the observation that zoiste + kyanite + paragonite + quartz assemblage is stable in this grade (Banno 1960; Enami 1980). This assemblage defines the minimum pressure of metamorphism,

which is about 8 Kb at 600 °C and 12 Kb at 700 °C (Fig. 8). The maximum pressure is estimated by calcite-aragonite transition (Boettcher and Wyllie 1967). Although aragonite-bearing rocks have been reported from a tectonic block emplaced in the Sanbagawa crystalline schists in the Kanto Mountains (Tanabe et al. 1982), calcite is stable throughout the Bessi area including the oligoclase-biotite zone (e.g., Wada et al. in prep.). Thus the temperature-pressure conditions of the oligoclase-biotite zone are semiquantitatively defined as the stippled area of Fig. 8.

Temperature: Coexisting compositions of muscovite-paragonite and garnet-biotite pairs allow temperature to be estimated for the oligoclase-biotite zone samples. The compositional gap between muscovite and paragonite in the celadonite-free system (X_{Na} = 0.30-0.91) discussed in the previous section gives a temperature of 600-650 °C on the solvus determined by Eugster et al. (1972). Temperature estimated with the garnet-biotite geothermometer is variable in some degree (Fig. 9). Temperature calculated by Pigage and Greenwood (1982) calibration is 610 ± 25 °C and corresponds well to that obtained by muscovite-paragonite pair. On the other hand, temperatures calculated with the Thompson (1976) and Ferry and Spear (1978) calibrations for the Ca- and Mn-free system are by 130 ± 10 °C lower than those with Pigage and Greenwood calibration. As suggested by Pigage and Greenwood, the Mg-Fe partition coefficient

between garnet and biotite is largely sensitive not only to temperature but also to X_{Ca} of garnet, and thus the low temperature estimations with the last two caliblations may result from the high X_{Ca} value of garnet in the Sanbagawa samples. Taking into account the equilibrium temperature of Mt. Higashi-akaishi peridotite (550-600 °C, Mori and Banno 1973; Yokoyama 1980), which occurs near the oligoclase-appearance line, the author deduces that the samples of the oligoclase-biotite zone were equilibrated at around 600 °C.

Pressure: Garnet + zoisite + plagioclase + quartz assemblage observed in pelitic schists may allow the caliblation of pressure at a given temperature. Reaction relation among these minerals is as follows:

$$4Ca_2Al_3Si_3O_{12}(OH) + SiO_2 = 5CaAl_2Si_2O_8 + Ca_3Al_2Si_3O_{12} + 2H_2O \quad \text{--- (1)}$$

zoisite quartz plagioclase garnet

The equilibrium constant is given by

$57782 - 103.658T + 1.445P + RT\ln K_s + 2RT\ln f_{H_2O} = 0$, where equilibrium constant $K_s = (a_{an}^{pl})^5 \cdot (a_{gr}^{ga})/(a_{zo}^{zo})^4$ (Ferry 1976), and a diagram of P_{solid}-P_{H_2O}-$\ln K_s$ relation at 600 °C can be illustrated in Fig. 10. The activity of anorthite in plagioclase (a_{an}^{pl}) was calculated with Models 2 and 4 proposed by Kerrick and Danken (1975). Activity coefficient (γ_{an}^{pl}) was estimated using the Margules parameters suggested by Newton et al. (1980) for the model 2, and a constant

γ_{an}^{pl} value of 1.28 (Orville 1972) was used for the model 4. The activity of grossular in garnet (a_{gr}^{ga}) was calculated assuming random mixing in the three 8-fold sites (i.e., $a_{gr}^{ga} = (\gamma_{gr}^{ga} \cdot X_{gr}^{ga})^3$), where γ_{gr}^{ga} was estimated by symmetric four-components solution model (Ganguly and Kennedy 1974) with the Margules parameters suggested by Ganguly (1979). For zoisite activity (a_{zo}^{zo}) was assumed as $X_{Al}^{Al(II)}$, because the Bessi zoisites are depleted in Fe^{3+} ($X_{Fe}{}^{3+}$ is less than 0.05) and Fe^{3+} is contained almost exclusively in the single Al(II) site (Ghose and Tsang 1971).

Pressure was calculated on seven zoisite-bearing samples (6 pelitic schists and 1 epidote amphibolite), and the result is shown in Table 3 and Fig. 10. The estimated pressure ranges from 9 to 11 Kb when $P_{H_2O} = P_{solid}$. The six pelitic schists examined do not contain calcite but graphite, and P_{H_2O} during the metamorphism may be somewhat lower than P_{solid} because of the presence of CO_2 in fluid (Itaya 1978). Thus the actual pressure may be slightly higher than that given in Table 3. Recent calibration of garnet-biotite-muscovite-plagioclase geobarometer (Ghent and Stout 1981) gives pressure of 9.3-10.6 Kb (Fig. 9).

The physical conditions of the oligoclase-biotite zone were estimated to be about 610 ± 25 °C and 10 ± 1 Kb, and are consistent with those estimated using the experimental results shown in Fig. 8.

Comparison with other metamorphic terrains

The temperature of the Sanbagawa oligoclase-biotite zone (or biotite zone of Higashino (1975)) approximates that for the New Caledonia omphacite zone of a typical high-pressure metamorphic terrain (Brothers and Yokoyama 1982) and the upper staurolite zone* of medium-pressure ones.

Oligoclase-biotite zone and omphacite zone: Comparison of mineral paragenesis of pelitic schists between Sanbagawa and New Caledonia has been discussed by Brothers and Yokoyama (1982).

They showed that garnet + glaucophane + omphacite assemblage occurs widely in pelitic schists of the New Caledonia omphacite zone, but Sanbagawa pelitic schists have commonly garnet + biotite + hornblende assemblage in the albite- and oligoclase-biotite zones. The garnet + glaucophane + omphacite assemblage was reported in quartz-free hornblende eclogites from the Iratsu mass (Enami et al. 1979), but glaucophane clearly postdated garnet + omphacite assemblage. Coexistence of these three minerals is probably unstable in the Sanbagawa metamorphic rocks, especially in pelitic schists having quartz ubiquitously.

The contrast of mineral assemblages between the two zones is shown in the A-F-M-C tetrahedron of Fig. 11a. Since the X_{Ca} value of plagioclase slightly differs between the two mineral zones, plagioclase is not an excess phase in rigorous application of the phase

rule and this figure is not quantitative. However, paragenetic relationship shown in this figure is revealed also in the comparison of samples of the Sanbagawa albite-biotite zone and the omphacite zone (cf. Table 4), in both of which albite is stable, and minor variation in X_{Ca} of plagioclase does not disturb the reaction relation proposed. Thus we may favor the view that the diagram adequately shows the assemblage difference between high-grade parts of the Sanbagawa and New Caledonia terrains. A generalized form for the reaction defining the transition between the two zones is

omphacite zone

garnet + glaucophane + omphacite + muscovite =

oligoclase-biotite zone

biotite + hornblende + plagioclase + quartz + H_2O --- (2)

Oligoclase-biotite zone and upper staurolite zone: Figs. 11b, c and d show critical assemblages in the Sanbagawa oligoclase-biotite zone and the upper staurolite zone of medium-pressure metamorphic terrains. A marked contrast in the set of mineral assemblages between the two mineral zones is that staurolite + biotite assemblage occurs commonly in the upper staurolite zone but is not stable in the Sanbagawa pelitic schists as discussed in the previous section. It is apparent from Figs. 11b and c that in the transition between the two mieneral zones two reactions are recognized to produce the staurolite + biotite assemblage. They are:

oligoclase-biotite zone

garnet + hornblende + paragonite + muscovite =

upper staurolite zone

staurolite + biotite + plagioclase + quartz + H_2O --- (3)

oligoclase-biotite zone

garnet + chlorite + paragonite + muscovite =

upper staurolite zone

staurolite + biotite + plagioclase + quartz + H_2O --- (4)

Reaction (3) represents more Ca-enriched rock bulk composition than reaction (4). In the oligoclase-biotite zone, garnet + chlorite + paragonite assemblage occurs in pelitic schists (sample OP-08), but Ca-richer pelitic schist having garnet + hornblende + paragonite assemblage is not confirmed. The reaction (4) may define a transition between the two mineral zones on ordinary pelitic schists.

Another possible reaction defining the boundary between the two mineral zones is

oligoclase-biotite zone

zoisite + paragonite + quartz =

upper staurolite zone

aluminum silicate + muscovite + plagioclase + H_2O --- (5)

As discussed by Banno (1960), this reaction suggests that in the oligoclase-biotite zone aluminum silicate is expected to occur only in

plagioclase-free rocks. In the Sanbagawa terrain plagioclase is ubiquitous in all pelitic schists; and this could explain why aluminum silicate is absent in the Sanbagawa pelitic schists, showing a marked contrast to common occurrences of aluminum silicate-bearing assemblages in medium-pressure metamorphic terrains.

Equation and dP/dT: The parameters in reactions (2), (3), (4) and (5) have been set according to the matrix calculation method (Brown 1971) and natural mineral compositions shown in Table 2 and reported in some literature. Basic assumptions made in setting up the equations are that H_2O is the only fluid component and there is no interchange of compositions except for H_2O interchance between the fluid and solid phases. The results of the calculations are shown in Table 4. Obviously the data in the table do not strictly represent natural values owing to the variations in mineral compositions. The calculations for different sets of mineral compositions, however, suggest that these reactions are applicable to various rock bulk compositions, and are generally representative.

The dP/dT values of the equations were calculated using the Clapeyron-Clausius equation on the following assumptions: (1) entropy change is considered for dehydration alone, (2) volume change is ΔV_{solid} at the standard state plus V_{H_2O} at selected T and P, and (3) $P_{H_2O} = P_{solid}$. Sets of temperature and pressure conditions arbitrarily selected for the dP/dT calculations are 600 °C and 10 Kb for the

reaction (2) and 600 °C and 7 Kb for the reactions (3), (4) and (5), respectively. The data used are listed in Table 5 and results of calculations are given in Table 4. There are some uncertainties in the dP/dT value calculated, which are mainly due to the difficulty of estimating mineral compositions reacted actually. However, it may be worthy to mention that the slops of the reactions are fairly gentle, especially for the reactions (2) and (3). This suggests that the contrasts of mineral assemblages related by these reactions result mainly from the difference in pressure during the metamorphism. Volume changes of these reactions show that the assemblages of the oligoclase-biotite zone are favored by higher-pressure condition than those of the upper staurolite zone, and show a lower-pressure equilibrium than those of the New Caledonia omphacite zone; These relationships support the estimated pressure conditions of these three mineral zones (oligoclase-biotite zone: 10 ± 1 Kb, this paper, upper staurolite zone: 5-6 Kb, Pigage 1976; Yardley et al. 1980; Pigage and Greenwood, 1982, omphacite zone: 12-14 Kb, Brothers and Yokoyama 1982). A combination of mineral assemblages shown in Fig. 7 represents a characteristic paragenesis of pelitic schists in the high-grade part of an intermediate high-pressure metamorphism.

Acknowledgements

The author wishes to express his sincere thanks to Profs. K. Suwa and S. Banno for their critical comments on the manuscript, and Dr.

T. Itaya for his kind advice on the ore microscopy. Thanks are also due to Messrs. I. Hiraiwa and S. Yogo who helped to prepare some thin sections.

Footnotes:

Page 3.

* The term " pelitic schists " in this study means black or gray micaceous metasediments containing carbonaceous materials. The carbonaceous materials are weak to well ordered graphite in the chlorite and garnet zones, and well ordered graphite in the biotite zone (Itaya, 1981).

** The occurrence of sodic plagioclase with X_{Ca} = 0.10-0.20 in the Sanbagawa terrain was once reported from the Bessi area by Miyashiro and Banno (1958), Hide (1961) and Banno (1964) using optical determinations. Later investigators (e.g., Ernst et al. 1970; Banno et al. 1976), who worked mainly in the areas east of the Bessi, did not recognize sodic plagioclase with $X_{Ca} > 0.04$ using electron-probe microanalysis. Thus it has been considered that oligoclase or more calcic plagioclase is absent in the Sanbagawa metamorphic rocks until the reconfirmation of them by Enami.

Page 16.

* Notable difference in X_{Mg} of chlorites could not be revealed between the two mineral assemblages. The chlorites occur as prismatic crystals forming a liniation and show a textural characterstic of primary phase, but their chemical composition may have been slightly changed in the retrogressive stage.

Page 22.

* The " upper staurolite zone " in this paper includes the staurolite-kyanite zone of Pigage (1976), upper staurolite zone of Yardley et al. (1980) and kyanite zone of Pigage and Greenwood (1982), in which the staurolite + aluminum silicate assemblage is stable in pelitic schists.

Appendix

Mineralogical data on constituent minerals of some samples discussed in the text other than the pelitic schists of the oligoclase-biotite zone are shown. Mineral assemblages and representative analyses of major constituents are given in Tables 1 and 2, respectively. Localities are shown in Fig. 2 in the text.

References

Banno, S. (1960) Notes on rock-forming minerals (12) Finding of paragonite from the Bessi district, Sikoku, and its paragenesis, J. Geol. Soc. Jpn., 66, 123-130

Banno, S. (1964) Petrologic studies on Sanbagawa crystalline schists in the Bessi-Ino district, central Sikoku, Japan, J. Fac. Sci. Univ. Tokyo, Sect. 2, 15, 203-319

Banno, S., Higashino, T., Otsuki, M., Itaya, T. and Nakajima, T. (1978) Thermal structure of the Sanbagawa metamorphic belt in central Shikoku, J. Phys. Earth, 26, Suppl., 345-356

Banno, S. and Kurata, H. (1972) Distribution of Ca in zoned garnet of low-grade pelitic schists, J. Geol. Soc. Jpn., 78, 507-512

Banno, S., Yokoyama, K., Iwata, O. and Terashima, S. (1976) Genesis of epidote amphibolite masses in the Sanbagawa metamorphic belt of central Shikoku, J. Geol. Soc. Jpn., 82, 199-210 (in Japanese with English abstract)

Bence, A. E. and Albee, A. L. (1968) Empirical correction factors for the electron microanalysis of silicates and oxides, J. Geol., 76, 382-403

Black, P. M. (1973a) Mineralogy of New Caledonian metamorphic rock I. Garnets from the Ouégoa district, Contrib. Mineral. Petrol., 38, 221-235

Black, P. M. (1973b) Mineralogy of New Caledonian metamorphic rocks II. Amphiboles from the Ouègoa district, Contrib. Mineral. Petrol., 39, 55-64

Black, P. M. (1974) Mineralogy of New Caledonian metamorphic rocks III. Pyroxenes, and major element partitioning between pyroxenes, amphiboles and garnets from the Ouègoa district, Contrib. Mineral. Petrol., 45, 281-288

Black, P. M. (1975) Mineralogy of New Caledonian metamorphic rocks IV. Sheet silicates from the Ouègoa district, Contrib. Mineral. Petrol., 49, 269-284

Black, P. M. (1977) Regional high-pressure metamorphism in New Caledonia: phase equilibria in the Ouègoa district, Tectonophysics, 43, 89-107

Boettcher, A. L. and Wyllie, P. J. (1967) Revision of the calcite-aragonite trangition, with the location of a triple point between calcite I, calcite II and aragonite, Nature, 213, 792-793

Brothers, P. N. and Yokoyama, K. (1982) Comparison of the high-pressure schist belts of New Caledonia and Sanbagawa, Japan, Contrib. Mineral. Petrol., 79, 219-229

Brown, E. H. (1971) Phase relations of biotite and stilpnomelane in the greenschists facies, Contrib. Mineral. Petrol., 31, 275-299

Burnham, C. W., Holloway, J. R. and Davis N. F. (1969) Thermodynamic properties of water to 1,000 °C and 10,000 bars, Geol. Soc. Am., Spec. Pap., 132, 96p

Coleman, R. G. and Lanphere, M. A. (1971) Distribution and age of high-grade blueschists, associated eclogites, and amphibolites from Oregon and California, Geol. Soc. Am. Bull., 82, 2397-2412

Coleman, R. G. and Papike, J. J. (1968) Alkali amphiboles from the blueschists of Cazadero, California, J. Petrol., 9, 105-122

Dodge, F. C. W., Smith, V. C. and Mays, R. E. (1969) Biotites from granitic rocks of the central Sierra Nevada batholith, California, J. Petrol., 10, 250-271

Enami, M. (1978) Petrological study of epidote amphibolites and basic schists in the Bessi area, Sanbagawa metamorphic terrain in central Shikoku, M. Sci. Thesis, Kanazawa Univ.

Enami, M. (1980) Notes on petrography and rock-forming mineralogy (8) Margarite-bearing metagabbro from the Iratsu mass in the Sanbagawa belt, central Shikoku, J. Jpn. Assoc. Mineral. Petrol. Econ. Geol., 75, 245-253

Enami, M. (1981) On sodic plagioclase in some rocks of the Sanbagawa metamorphic belt in the Bessi district, Shikoku, Japan, Proc. Jpn. Acad., Ser.B, 57, 188-193

Enami, M. (1982) Oligoclase-biotite zone of the Sanbagawa metamorphic terrain in the Bessi district, central Shikoku, Japan, J. Geol. Soc. Jpn., 88, 887-900 (in Japanese with English abstract)

Enami, M., Iwata, O. and Banno, S. (1979) Notes of petrography and rock-forming mineralogy (6) Glaucophane in the Iratsu amphibolite in the Sanbagawa belt in central Shikoku, J. Jpn. Assoc. Mineral. Petrol. Econ. Geol., 74, 332-338

Ernst, W. G. (1963) Significance of phengitic micas from low-grade schists, Am. Mineral., 48, 1357-1373

Ernst, W. G. (1973) Interpretative synthesis of metamorphism in the Alps, Geol. Soc. Am. Bull., 84, 2053-2078

Ernst, W. G. (1977) Mineralogic study of eclogitic rocks from Alpe Arami, Lepontine Alps, southern Switzerland, J. Petrol., 18, 371-398

Ernst, W. G., Seki, Y., Onuki, H. and Gilbert, M. C. (1971) Comparative study of low-grade metamorphism in the California Coast Ranges and the outer metamorphic belt of Japan, Geol. Soc. Am. Mem., 124, 276p

Eugster, H. P., Albee, A. L., Bence, A. E., Thompson, J. B., Jr. and Waldbaum, D. R. (1972) The two-phase region and excess mixing properties of paragonite-muscovite crystalline solutions. J. Petrol., 13, 147-179

Ferry, J. M. (1976) P, T, f_{CO_2}, and f_{H_2O} during metamorphism of calcareous sediments in the Waterville-Vassalboro area, south-central Main, Contrib. Mineral. Petrol., 57, 119-143

Ferry, J. M. and Spear F. S. (1978) Experimental caliburation of the partitioning of Fe and Mg between biotite and garnet, Contrib. Mineral. Petrol., 66, 113-117

Franz, G. and Althaus, E. K. (1977) The stability relations of paragenesis paragonite-zoisite-quartz, Neues. Jahrb. Mineral. Abh., 130, 159-167

Fyfe, W. S., Turner, F. J. and Verhoogen, J. (1958) Metamorphic reactions and metamorphic facies, Geol. Soc. Am. Mem., 73, 259p

Ganguly, J. (1979) Garnet and clinopyroxene solid solutions, and geothermometry based on Fe-Mg distribution coefficient, Geochim. Cosmochim. Acta, 43, 1021-1029

Ganguly, J. and Kennedy, G. C. (1974) The energetics of natural garnet solid solution I. Mixing of the aluminosilicate end-members, Contrib. Mineral. Petrol., 48, 137-148

Ghent E. D. and Stout, M. Z. (1981) Geobarometry and geothermometry of plagioclase-biotite-garnet-muscovite assemblages, Contrib. Mineral. Petrol., 76, 92-97

Ghose, S. and Tsang, T. (1971) Ordering of V^{2+}, Mn^{2+} and Fe^{3+} irons in zoisite, $Ca_2Al_3Si_3O_{12}(OH)$, Science, 171, 374-376

Griffen, D. T. and Ribbe, P. H. (1973) The crystal chemistry of staurolite, Am. J. Sci., 273A, 479-495

Guidotti, C. V. (1974) Transition from staurolite to sillmanite zone, Rangeley Quadrangle, Maine, Geol. Soc. Am. Bull., 85, 475-490

Hey, M. H. (1954) A new review of the chlorites, Mineral. Mag., 30, 277-292

Hide, K. (1961) Geologic structure and metamorphism of the Sanbagawa crystalline schists of the Besshi-Shirataki mining district in Shikoku, Southwest Japan, Geol. Rep. Hiroshima Univ., 9, 1-87 (in Japanese with English abstract)

Higashino, T. (1975) Biotite zone of the Sanbagawa metamorphic terrain in the Shiragayama area, central Shikoku, Japan, J. Geol. Soc. Jpn., 81, 653-670 (in Japanse with English abstract)

Higashino, T., Sakai, C., Otsuki, M., Itaya, T. and Banno, S. (1981) Electron microprobe analyses of rock-forming minerals from the Sanbagawa metamorphic rocks, Shikoku Part I. Asemi river area, Sci. Rep. Kanazawa Univ., 26, 73-122

Hiramura, M. (1978) Notes on petrography and rock-forming mineralogy (2) Find of a paragonite-bearing quartz schist from the Kotu district, eastern Shikoku, J. Jpn. Assoc. Mineral. Petrol. Econ. Geol., 73, 152-154

Holland, T. J. B. (1979) Experimantal determination of the reaction paragonite = jadeite + kyanite + H_2O, and internally consistent thermodynamic data for part of the system Na_2O-Al_2O_3-SiO_2-H_2O, with applications to eclogites and blueschists, Contrib. Mineral. Petrol., 68, 293-301

Itaya, T. (1978) Sulfide and oxide minerals, sphene and carbonaceous matter in the Sanbagawa metamorphic rock, and their roles in metamorphism, Ph. D. Thesis, Tohoku Univ.

Itaya, T. (1981) Carbonaceous material in pelitic schists of the Sanbagawa metamorphic belt in central Shikoku, Japan, Lithos, 14, 215-224

Kerrick, D. M. and Darken, L. S. (1975) Statistical thermodynamic models for ideal oxide and silicate solid solutions, with application to plagioclase, Geochim, Cosmochim. Acta, 39, 1431-1442

Kojima, G., Hide, K. and Yoshino, G. (1956) The stratigraphical position of Kieslager in the Sanbagawa crystalline schists zone in Shikoku, J. Geol. Soc. Jpn., 62, 30-45 (in Japanse with English abstract)

Kunugiza, K. (1980) Dunites and serpentinites in the Sanbagawa metamorphic belt, central Shikoku and Kii Peninsula, Japan, J. Jpn. Assoc. Mineral. Petrol. Econ. Geol., 75, 14-20

Kurata, H. (1972) Local chemical heterogeneity of chlorites in Sanbagawa pelitic schists from the Sazare area, central Shikoku, J. Geol. Soc. Jpn., 78, 653-657

Kurata, H. and Banno, S. (1974) Low-grade progressive metamorphism of pelitic schists of the Sazare area, Sanbagawa metamorphic terrain in central Shikoku, Japan, J. Petrol., 15, 361-382

Miyashiro, A. (1961) Evolution of metamorphic belts, J. Petrol., 2, 277-331

Miyashiro, A. and Banno, S. (1958) Nature of glaucophanitic metamorphism, Am. J. Sci., 256, 97-110

Mori, T. and Banno, S. (1973) Petrology of peridotite and garnet clinopyroxenite of the Mt. Higashi-akaishi mass, central Shikoku, Japan - Subsolidus relation of anhydrous phases, Contrib. Mineral. Petrol., 41, 301-323

Newton, R. C., Charlu, T. V. and Kleppa, O. J. (1980) Thermochemistry of the high structural state plagioclases, Geochim. Cosmochim. Acta, 44, 933-941

Orville, P. M. (1972) Plagioclase cation exchange equilibria with aqueous chloride solution: results at 700 °C and 2,000 bars in the presence of quartz, Am. J. Sci. 272, 234-272

Perkins, D., III, Westrum, E. F., Jr. and Essene, E. J. (1980) The thermodynamic properties and phase relations of some minerals in the system $CaO-Al_2O_3-SiO_2-H_2O$, Geochim. Cosmochim. Acta, 44, 61-84

Pigage, L. C. (1976) Metamorphism of Settler schist, southwest of Yale, British Columbia, Can. J. Earth Sci., 13, 405-421

Pigage, L. C. and Greenwood, H. J. (1982) Internally consistent estimates of pressure and temperature: the staurolite problem, Am. J. Sci., 282, 943-969

Platt, J. P. (1975) Metamorphic and deformational processes in the Franciscan complex, California: some insights from the Cataline schist terrane, Geol. Soc. Am. Bull., 86, 1337-1347

Robie, R. A., Bethke, P. M. and Beardsley, K. M. (1967) Selected X-ray crystallographic data molar volumes, and densities of minerals and related substances, U. S. Geol. Surver Bull., 87p

Takasu, A. and Makino, K. (1980) Stratigraphy and geologic structure of the Sanbagawa metamorphic belt in the Bessi district, Shikoku, Japan - Peexamination of the recumbent fold structures -, Earth Sci. (Chikyu Kagaku), 34, 16-26 (in Japanese with English abstract)

Tanabe, K., Tomioka, N. and Kanehira, K. (1982) Jadeite-aragonite-bearing rocks from the Sanbagawa metamorphic terrane in the Kanto Mountains, Proc. Jpn. Acad., Ser. B, 58, 199-203

Thompson, A. B., Jr. (1976) Mineral reactions in pelitic rocks: II. Calculation of some P-T-X(Fe-Mg) phase relations, Am. J. Sci., 276, 425-454

Yardley, B. W. D., Leake, B. E. and Farrow, C. M. (1980) The metamorphism of Fe-rich pelites from Connemara, Ireland, J. Petrol., 21, 365-399

Yokoyama, K. (1980) Nikubuchi peridotite body in the Sanbagawa metamorphic belt; thermal history of the 'Al-pyroxene-rich suite' peridotite body in high pressure metamorphic terrain, Contrib. Mineral. Petrol., 73, 1-13

Yusa, Y. (1975) A rapid method for quantitative microprobe analysis of olivines, pyroxenes and feldspars, J. Jpn. Assoc. Mineral. Petrol. Econ. Geol., 70, 141-156

Caption for Figure

Fig. 1. Geological sketch map of the Sanbagawa terrain in central Shikoku (mofified from Fig. 1 of Mori and Banno (1973)).
TO: Tonaru mass, HA: Higashi-akaishi mass, IR: Iratsu mass.

Fig. 2. Metamorphic zonation map of the Sanbagawa terrain in the Bessi area (Banno et al. 1978; Enami 1982). Broken line shows the lithologic boundary between epidote amphibolite masses and the surrounding crystalline schists.

Fig. 3. Stabilities of minerals in pelitic schists (Banno 1964; this study). Note that not all the minerals in the figure occur in the same sample. Solid line: major constituent, dashed line: minor constituent. Quartz is always associated. Paragonite occurs in the oligoclase-biotite zone, but is not confirmed from the other mineral zones.

Fig. 4. Composition of biotite in the Fe-Mg-Al^{VI} diagram.

Fig. 5. X_{Na}-X_{Si} relationships of coexisting muscovite and paragonite. Samples are grouped by metamorphic grade. Oligoclase-biotite zone: Enami (1978, this study), Albite-biotite zone: Enami (1978), Garnet zone: Hiramura (1978), Higashino et al. (1981), Enami (new data).

Fig. 6. Comparison of mineral compositions for various assemblages.
(a): X_{Mg} values of garnet, biotite, chlorite and hornblende.
(b): X_{Mg}-X_{Ca} relationship of garnet.

Fig. 6 (continued).

Abbreviations for minerals. G: garnet, B: biotite, H: hornblende, C: chlorite, P: paragonite. Assemblages (7) and (8) are from epidote amphibolite (sample AE-01) and basic schist (sample OB-01), respectively, and others are from pelitic schists in the oligoclase biotite zone (see text and appendix).

Fig. 7. Paragenetic relationships in pelitic schists of the oligoclase-biotite zone plotted in the A-F-M-C tetrahedron. Note that staurolite is plotted on the Al- or Ca-rich side of the garnet - hornblende-paragonite plane. Abbreviations for minerals are defined in Tables 1 and 4.

Fig. 8. Temperature and pressure ranges of the oligoclase-biotite zone (stippled) estimated by using reference equilibrium curves with $P_{H_2O} = P_{solid}$. Curve 1: Boettcher and Wyllie (1967), 2: Holland (1979), 3, 4 and 5: Perkins et al. (1980), 6: Frantz and Althaus (1977).

Fig. 9. Calculated metamorphic conditions using garnet-biotite geothermometry and garnet-biotite-muscovite-plagioclase geobarometry. Temperature. 1: Thompson (1976), 2: Ferry and Spear (1978), 3: Pigage and Greenwood (1982). Equilibrium pressure was assumed as 10 Kb for all the samples. Pressure. Ghent and Stout (1981). Equilibrium temperature was assumed as 600 °C fo all the samples.

Fig. 10. P_{H_2O}-P_{solid}-ln K_s diagram for the reaction (1) at 600 °C. Fugacity coefficients of H_2O are from Burnham et al. (1969). (1) and (2) are models 2 and 4 of Kerrick and Darken (1975), respectively.

Fig. 11. Peaction relations of pelitic schist assemblages from the Sanbagawa oligoclase-biotite zone (SO zone), New Caledonia omphacite zone (NO zone) and upper staurolite zone (US zone) of medium-pressure metamorphic terrains. Excess phases are quartz, plagioclase and muscovite for (a), (b) and (c), and quartz for (d). Abbreviations for minerals are defined in Tables 1 and 4.

Caption for Table

Table 1. Mineral assemblages of pelitic schists in the oligoclase-biotite zone. Tourmaline, apatite and allanite occur as accesaries. Abbreviations for minerals. Ca: garnet, Bi: biotite, Hb: hornblende, Ch: chlorite, Pa: paragonite, Ms: muscovite, Cz: clinozoisite, Zo: zoisite, Pl: plagioclase, Qz: quartz, Sp: sphene, Cc: calcite, Il: ilmenite, Ru: rutile, Po: pyrrhotite, Py: pyrite, Cp: chalcopyrite, Cm: well ordered graphite.

Table 2. Chemical compositions of major constituent minerals in pelitic schists of the oligoclase-biotite zone. *total iron iron as FeO. Abbreviations for minerals are defined in Table 1.

Table 3. Plagioclase, garnet and zoisite composition and estimates of pressure.

For garnet, $X_i = i/(Fe + Mg + Mn + Ca)$. For zoisite $X_{Al} = Al/(Al + Fe^{3+})$. For plagioclase, see text. * Calculated pressure using different activity model for plagioclase.

(1) and (2) are models 2 and 4 of Kerrick and Darken (1975), respectively. Equilibrium temperature was assumed as 600 °C for all the samples. Sample OE-02: epidote amphibolite (see appendix).

Table 4. Molar coefficients of minerals, ΔV and dP/dT in reactions (2), (3), (4) and (5).

Negative coefficients indicate low temperature side minerals.

* 1: sample 10717, Black (1973a, b, 1974). Muscovite data is from sample 10741 (Black 1975), 2: sample TH71081303 (Higashino et al. 1981), 3: sample 373 (Pigage and Greenwood 1982), 4: sample BL2915E (Yardley et al. 1980), 5: sample III-6 (Pigage 1976). Data of sample OE-01 are given in appendix.

Abbreviations for minerals. Gl: glaucophane, Om: omphacite, St: staurolite, As: aluminum silicates. Others are defined in Table 1.

Table 5. Data used in calculation of dP/dT.

* 1: From Robie et al. (1967), 2: Calculated from cell dimensions of minerals of similar composition given in literature (biotite:

Table 5 (continued).

Dodge et al. 1969, glaucophane: Coleman and Papike 1968, staurolite: Griffen and Ribbe 1973, muscovite: Ernst 1963), 3: Calculated from cell dimensions ontained by the X-ray powder method, 4: Calculated from specific gravity estimated with specific gravity-composition diagram in Hey (1954, Fig. 4), 5: From Black (1977), 6: From Burnham et al. (1969), 7: Extrapolated values of the data in Fyfe et al. (1958). Numbers in parantheses indicate those of reactions in the text.

Appendix

Table 1. Mineral assemblages of epidote amphibolites and basic and pelitic schists. Abbreviations for minerals: Mc: microcline, others are defined in Table 1 in the text. Abbreviations for rock types: Bs: basic schist, Ea: epidote amphibolite, Ps: pelitic schist.

Table 2. Chemical compositions of major constituent minerals. * total iron as FeO. Abbreviations for minerals are defined in Table 1 of the text and appendix.

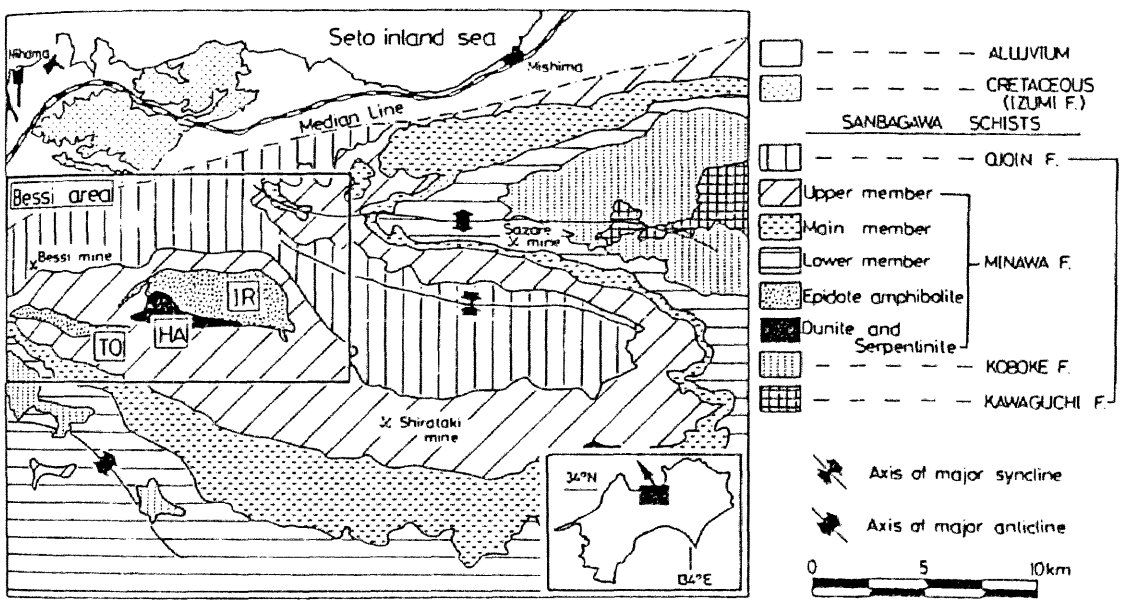

Fig. 1. Geological sketch map of the Sanbagawa terrain in central Shikoku.

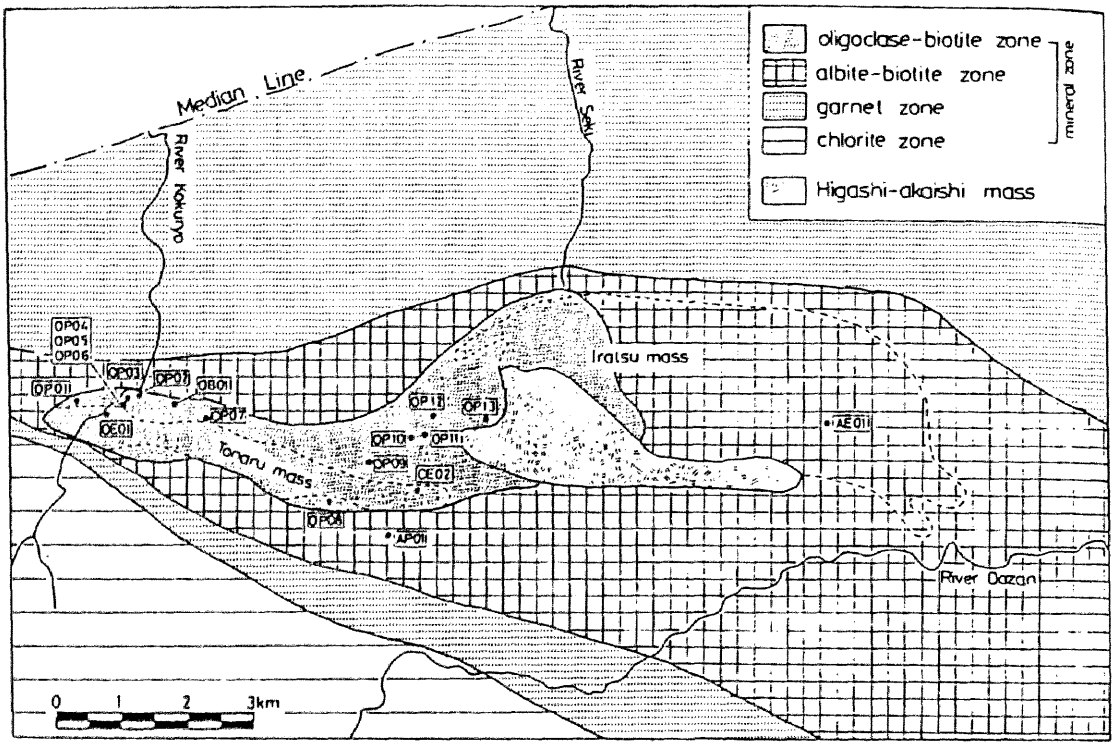

Fig. 2. Metamorphic zonation map of the Sanbagawa terrain in the Bessi area.

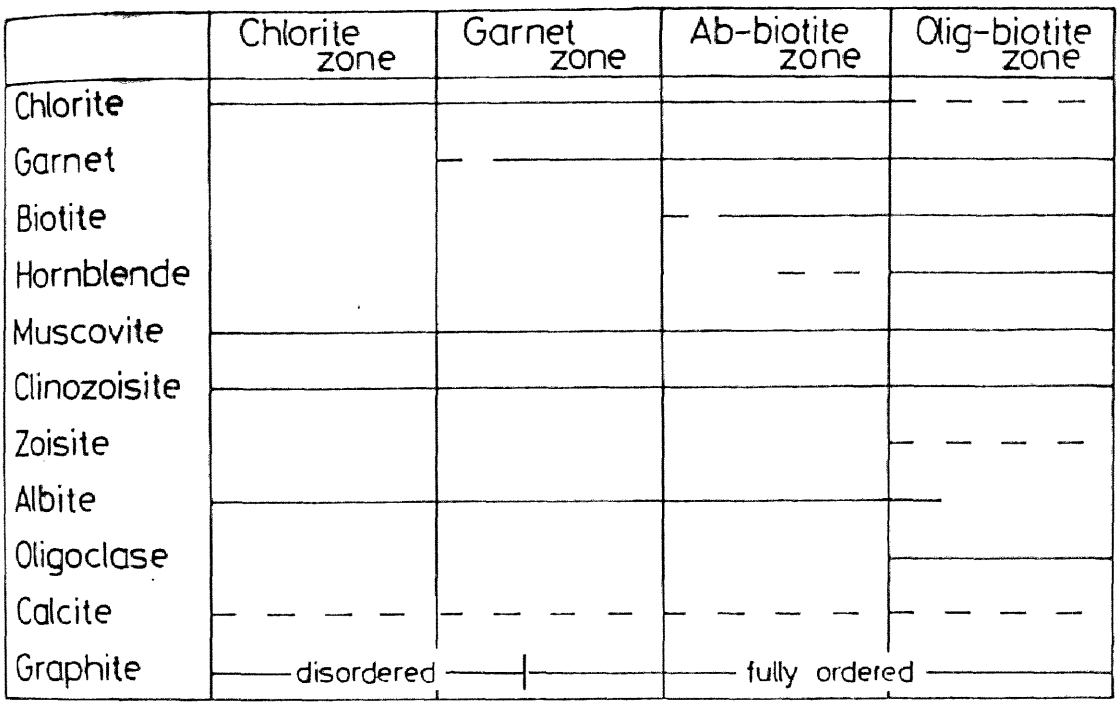

Fig. 3. Stabilities of minerals in pelitic schists.

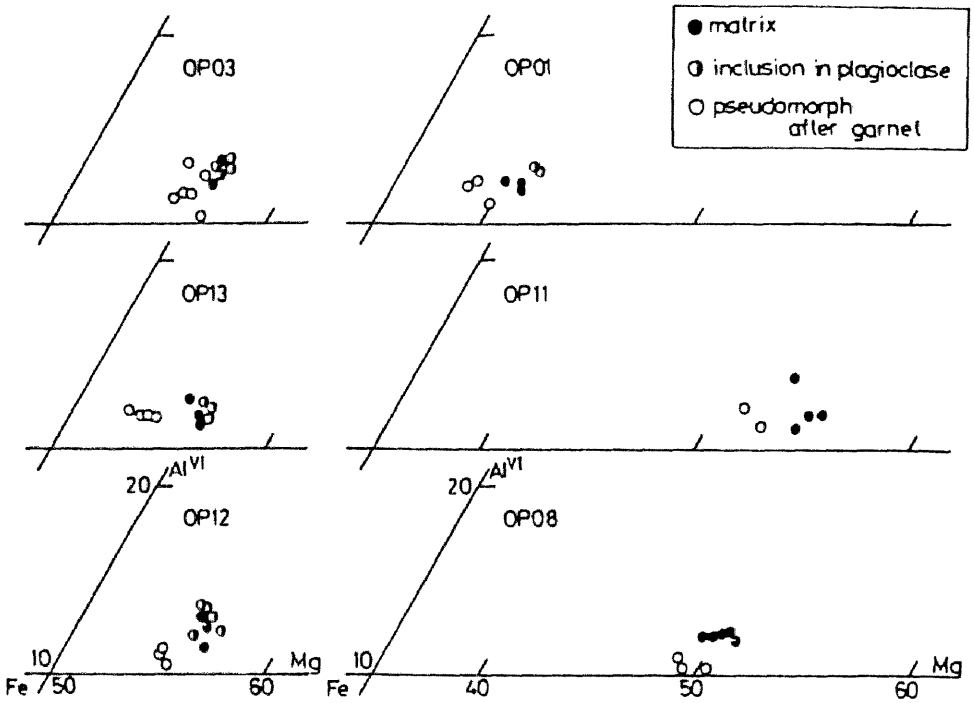

Fig. 4. Composition of biotite in the Fe-Mg-Al^{VI} diagram.

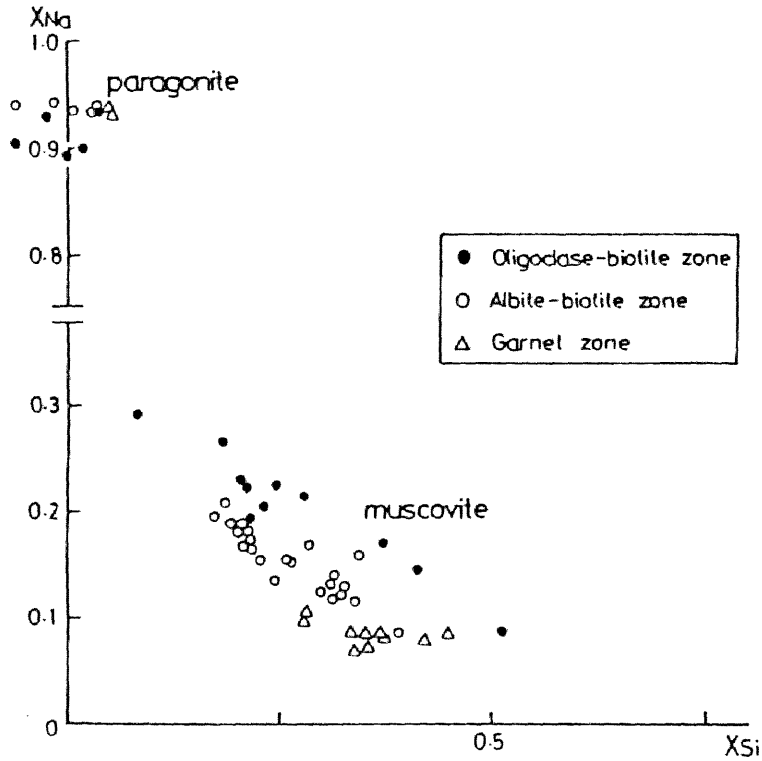

Fig. 5. X_{Na}-X_{Si} relationships of coexisting muscovite and paragonite.

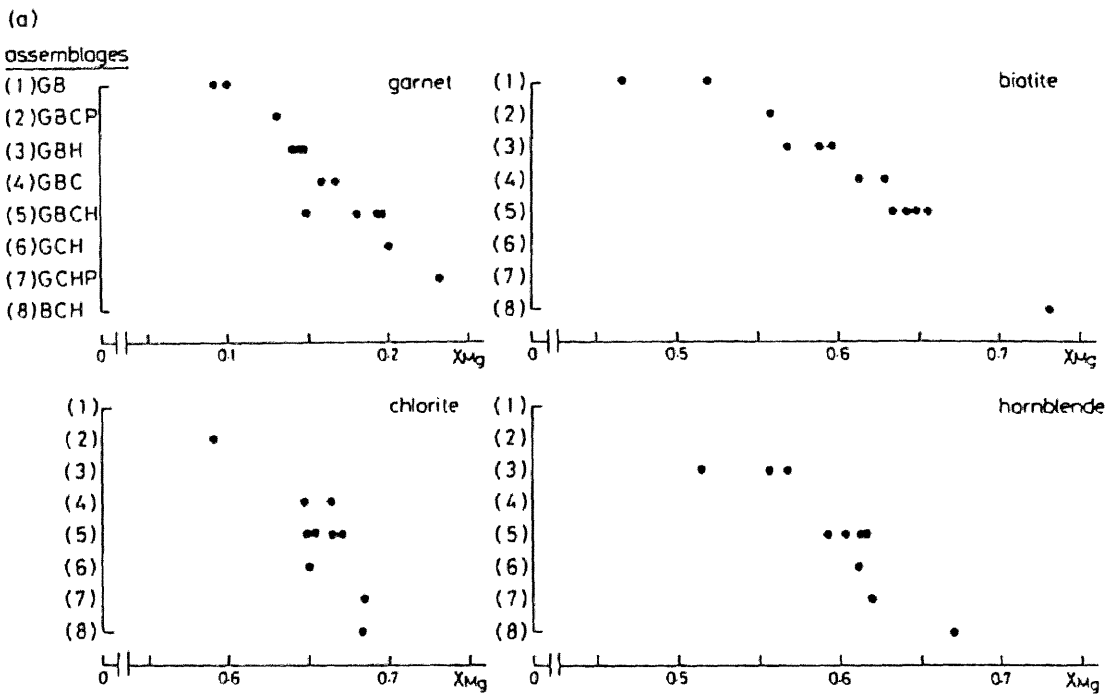

Fig. 6. Comparison of mineral compositions for various assemblages.

(a): X_{Mg} values of garnet, biotite, chlorite and hornblende.

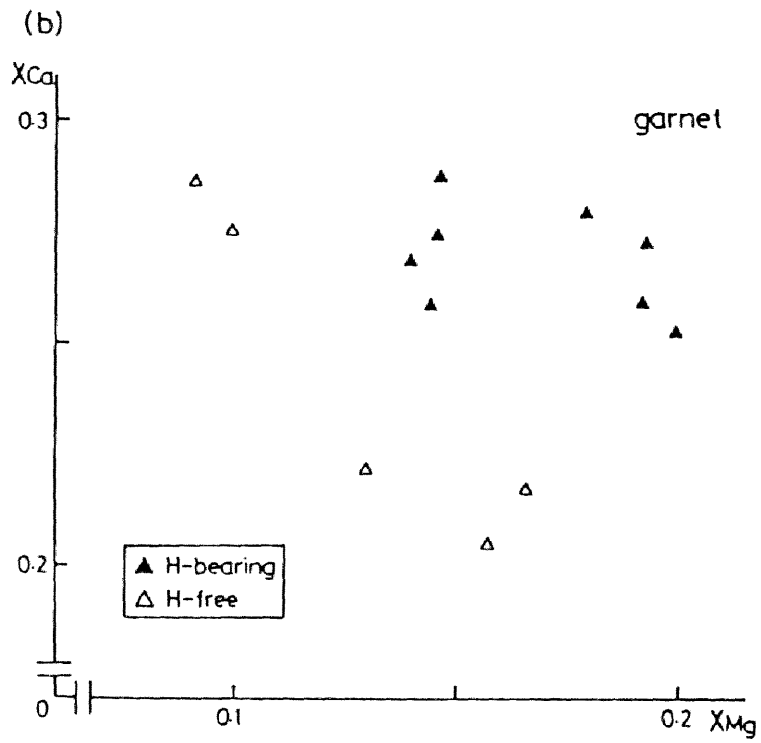

Fig. 6. Comparison of mineral compositions for various assemblages.

(b): X_{Mg}-X_{Ca} relationship of garnet.

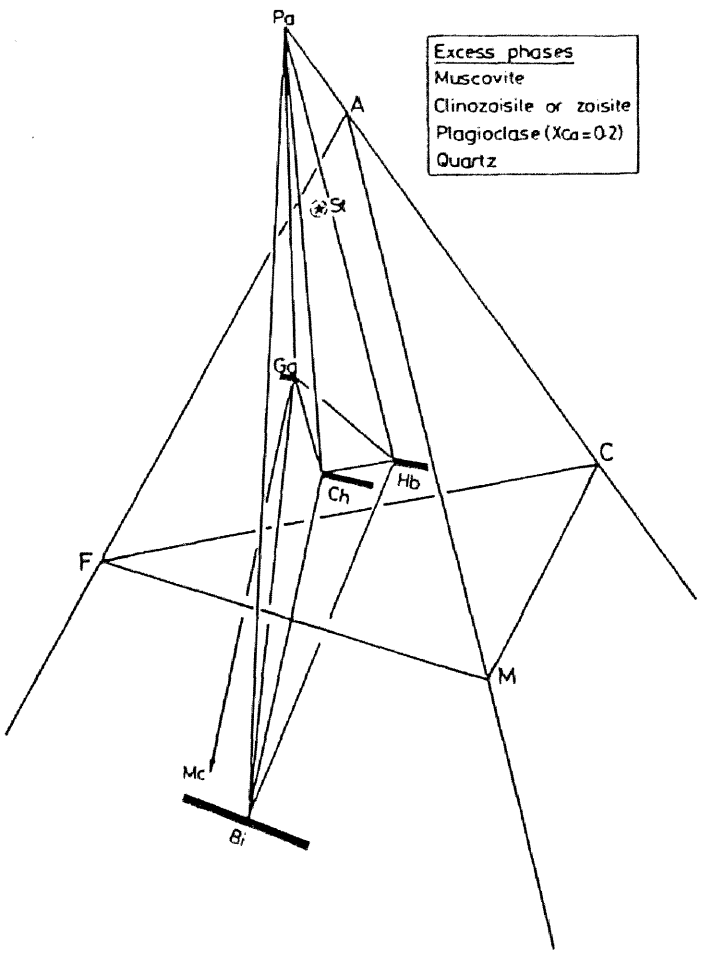

Fig. 7. Paragenetic relationships in pelitic schists of the oligoclase-biotite zone plotted in the A-F-M-C tetrahedron.

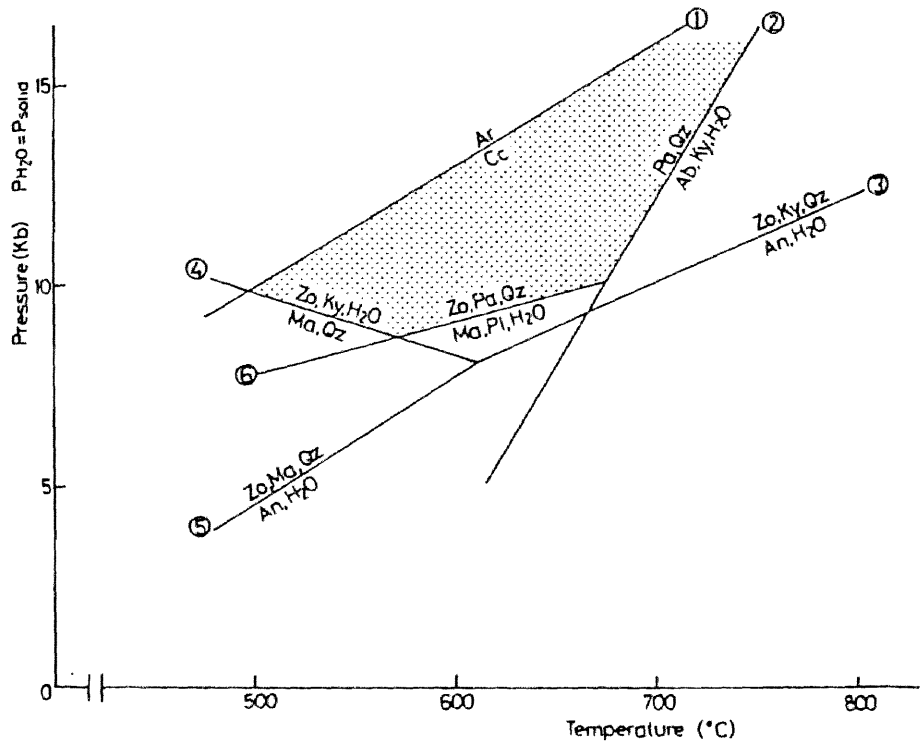

Fig. 8. Temperature and pressure ranges of the oligoclase-biotite zone (stippled) estimated by using reference equilibrium curves with $P_{H_2O} = P_{solid}$.

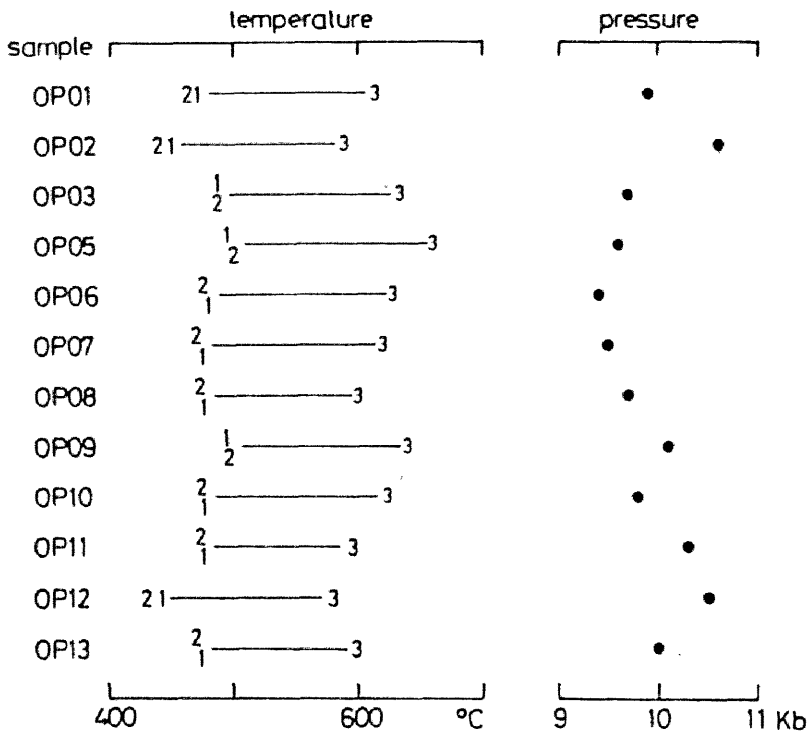

Fig. 9. Calculated metamorphic conditions using garnet-biotite geothermometry and garnet-biotite-muscovite-plagioclase geobarometry.

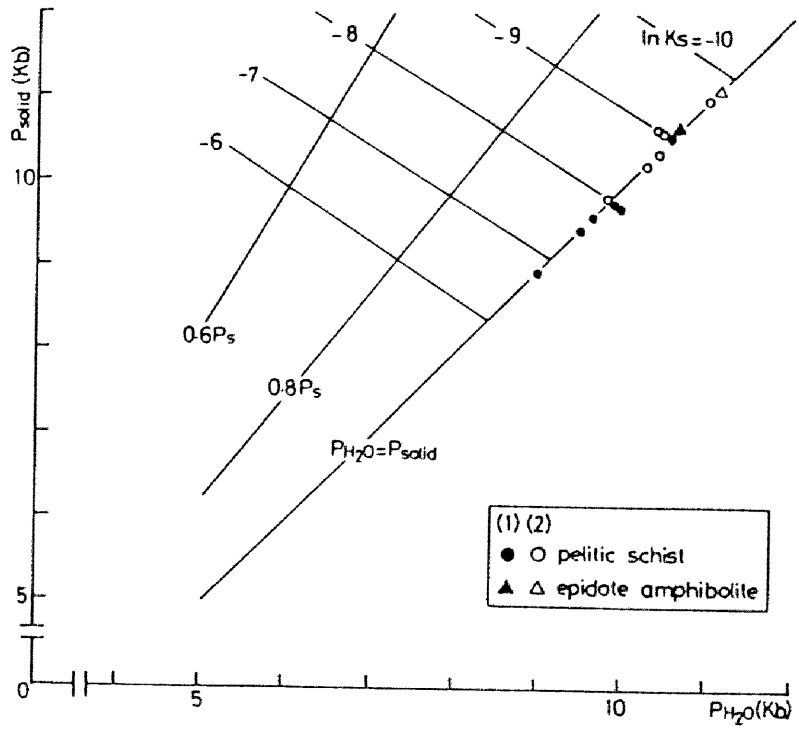

Fig. 10. P_{H_2O}-P_{solid}-ln K_s diagram for the reaction (1) at 600 °C.

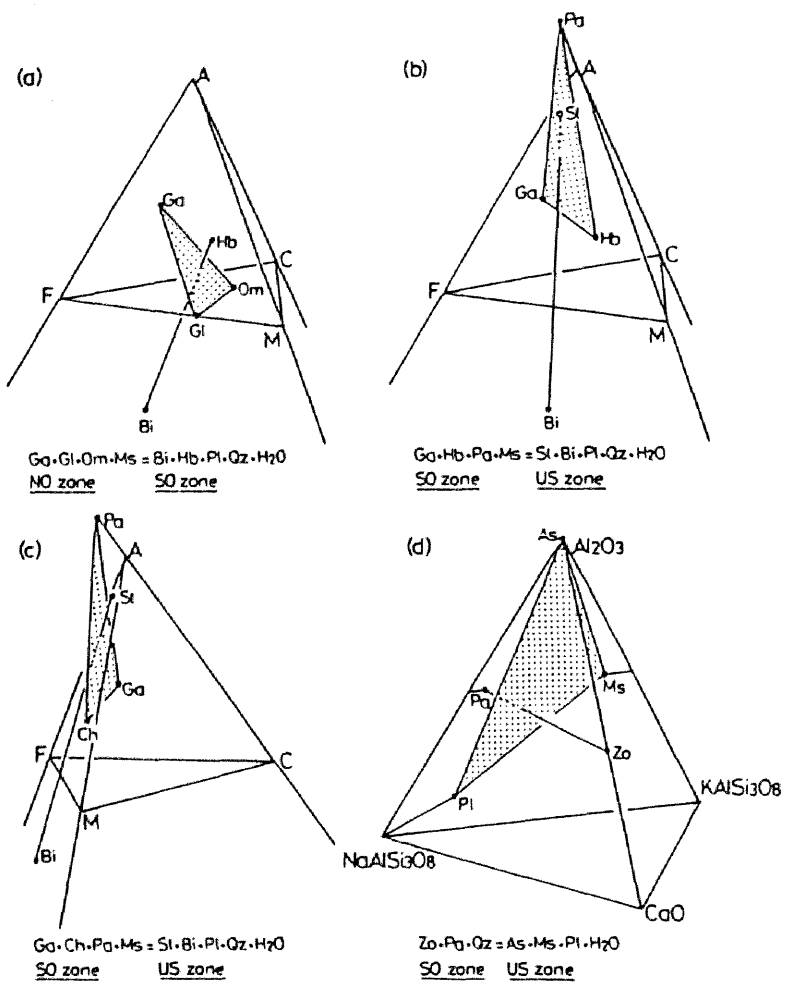

Fig. 11. Reaction relations of pelitic schist assemblages from the Sanbagawa oligoclase-biotite zone, New Caledonia omphacite zone and upper staurolite zone of medium-pressure metamorphic terrains.

Table 1. Mineral assemblages of pelitic schists in the oligoclase-biotite zone.

Sample	Ga	Bi	Hb	Ch	Pa	Ms	Cz	Zo	Pl	Qz	Sp	Cc	Il	Ru	Po	Py	Cp	Cm
OP-01	+	+				+	+		+	+	+		+	+	+			+
OP-02	+	+				+	+		+	+	+			+				+
OP-03	+	+	+	+		+	+	+	+	+	+			+	+	+		+
OP-04	+		+	+		+	+	+	+	+				+	+	+		+
OP-05	+	+	+	+		+	+	+	+	+				+	+	+		+
OP-06	+	+	+	+		+	+	+	+	+	+			+	+		+	+
OP-07	+	+	+			+	+	+	+	+	+			+		+	+	+
OP-08	+	+		+	+	+	+		+	+	+			+				+
OP-09	+	+	+			+	+		+	+	+			+	+			+
OP-10	+	+	+			+	+	+	+	+	+			+	+		+	+
OP-11	+	+		+		+	+		+	+	+			+				+
OP-12	+	+	+	+		+	+		+	+	+	+		+	+	+	+	+
OP-13	+	+		+		+	+		+	+	+			+	+			+

Enami
Table 1.

Table 2. Chemical compositions of major constituent minerals.

Sample	OP-02		OP-04		
Mineral	Ga	Bi	Ga	Hb	Ch
SiO_2	37.8	37.5	38.3	44.1	28.9
TiO_2		1.84		0.55	
Al_2O_3	21.4	16.5	21.1	15.1	19.2
FeO*	28.6	18.9	26.0	12.4	19.8
MnO	1.12	0.03	1.47	0.08	0.21
MgO	1.77	11.4	3.62	10.9	20.4
CaO	9.75	0.01	8.94	11.2	0.01
Na_2O		0.05		2.32	
K_2O		8.27		0.50	
Total	100.4_4	94.5_0	99.4_3	97.1_5	88.5_2
Si	2.997	5.687	3.027	6.463	5.827
Al^{IV}	0.003	2.313		1.537	2.173
Al^{VI}	1.996	0.635	1.965	1.070	2.389
Ti		0.210		0.061	
Fe^{2+*}	1.896	2.396	1.718	1.519	3.338
Mn	0.075	0.004	0.098	0.010	0.036
Mg	0.209	2.575	0.426	2.379	6.127
Ca	0.828	0.002	0.757	1.758	0.002
Na		0.015		0.659	
K		1.599		0.093	

Table 2. Chemical compoistions of major constituent minerals (continued).

Sample	OP-06				OP-07		
Mineral	Ga	Bi	Hb	Ch	Ga	Bi	Hb
SiO_2	38.5	38.4	42.6	27.6	38.3	38.8	44.7
TiO_2		1.48	0.52			1.81	0.53
Al_2O_3	21.2	17.4	16.0	19.4	21.1	17.1	15.8
FeO*	26.2	13.8	12.2	19.5	26.6	15.7	13.6
MnO	0.98	0.07	0.12	0.13	1.07	0.07	0.05
MgO	3.20	14.2	11.0	20.4	2.56	13.0	9.61
CaO	9.96	0.00	11.1	0.03	9.51	0.00	10.8
Na_2O		0.19	2.31			0.14	2.40
K_2O		8.44	0.63			8.67	0.48
Total	100.0_4	93.9_8	96.4_8	87.0_6	99.1_4	95.2_9	97.9_7
Si	3.027	5.705	6.302	5.669	3.043	5.738	6.505
Al^{IV}		2.295	1.698	2.331		2.262	1.495
Al^{VI}	1.964	0.751	1.091	2.364	1.975	0.718	1.214
Ti		0.165	0.058			0.201	0.058
Fe^{2+*}	1.722	1.714	1.509	3.348	1.767	1.941	1.655
Mn	0.065	0.009	0.015	0.023	0.072	0.009	0.006
Mg	0.375	3.142	2.424	6.241	0.303	2.864	2.083
Ca	0.839	0.000	1.759	0.007	0.809	0.000	1.683
Na		0.055	0.662			0.040	0.677
K		1.599	0.119			1.635	0.089

Table 2. Chemical compositions of major constituent minerals (continued).

Sample	OP-08					OP-13		
Mineral	Ga	Bi	Ch	Pa	Ms	Ga	Bi	Ch
SiO_2	37.4	37.5	25.7	46.9	48.9	37.0	37.0	28.4
TiO_2		1.74		0.05	0.45		1.36	
Al_2O_3	21.1	16.7	21.2	39.7	32.8	21.2	17.4	18.4
FeO*	28.9	17.2	22.2	0.24	1.56	28.5	14.5	19.7
MnO	1.16	0.05	0.07	0.00	0.00	1.41	0.03	0.11
MgO	2.42	12.2	18.0	0.12	1.67	3.19	14.0	20.3
CaO	7.65	0.00	0.00	0.11	0.00	7.72	0.00	0.00
Na_2O		0.03		7.26	1.55		0.13	
K_2O		8.38		0.75	8.58		8.75	
Total	98.6_3	93.8_0	87.1_7	95.1_3	95.5_1	99.0_2	93.1_7	86.9_1
Si	3.011	5.686	5.358	5.997	6.434	2.970	5.594	5.842
Al^{IV}		2.314	2.642	2.003	1.566	0.030	2.406	2.158
Al^{VI}	2.002	0.670	2.566	3.979	3.519	1.975	0.694	2.302
Ti		0.198		0.005	0.045		0.155	
Fe^{2+*}	1.945	2.180	3.869	0.026	0.172	1.912	1.833	3.388
Mn	0.079	0.006	0.012	0.000	0.000	0.096	0.004	0.019
Mg	0.290	2.755	5.590	0.023	0.327	0.381	3.153	6.200
Ca	0.660	0.000	0.000	0.015	0.000	0.664	0.000	0.000
Na		0.009		1.799	0.395		0.038	
K		1.620		0.122	1.439		1.687	

Table 3. Plagioclase, garnet and zoisite compositions and estimates of pressure.

	Pl	Ga				Zo	ln Ks		P (Kb)*	
Sample	X_{Ca}	X_{Fe}	X_{Mg}	X_{Mn}	X_{Ca}	X_{Al}	(1)	(2)	(1)	(2)
OP-03	0.23	0.57	0.14	0.03	0.26	0.96	-8.0	-9.0	9.8	10.5
OP-04	0.23	0.57	0.15	0.03	0.25	0.95	-7.7	-8.8	9.6	10.4
OP-05	0.23	0.54	0.13	0.06	0.27	0.95	-7.5	-8.6	9.5	10.3
OP-06	0.27	0.57	0.13	0.02	0.28	0.96	-6.8	-8.0	8.9	9.8
OP-07	0.23	0.60	0.10	0.02	0.28	0.97	-8.0	-9.0	9.8	10.5
OP-10	0.19	0.61	0.10	0.02	0.27	0.95	-9.0	-9.7	10.5	11.0
OE-02	0.18	0.62	0.07	0.02	0.29	0.95	-9.1	-9.8	10.6	11.1

Enami
Table 3.

Table 4. Molar coefficients of minerals, ΔV and dP/dT in reactions (2), (3), (4) and (5).

Reaction (2)	Olig-biotite zone					Omphacite zone				ΔV	dP/dT
Samples	Bi	Hb	Pl	Qz	H_2O	Ga	Gl	Om	Ms	(cm^3)	(bar/deg)
OP-07, BL-01 *1	0.88	0.15	3.82	1.11	1.00	-0.06	-0.80	-2.22	-1.06	76	6.3
OP-09, BL-01	0.99	0.54	4.54	1.77	1.00	-0.34	-1.07	-3.09	-1.23	97	5.0
TH-01 *2, BL-01	1.36	2.50	8.30	0.60	1.00	-0.87	-3.00	-6.91	-1.66	184	2.6

Reaction (3)	Olig-biotite zone				Upper staurolite zone						
Samples	Ga	Hb	Pa	Ms	St	Bi	Pl	Qz	H_2O		
OE-01, PG-01 *3	-0.40	-0.12	-0.62	-0.24	0.32	0.26	1.63	0.23	1.00	27	19
OE-01, YA-01 *4	-0.72	-0.09	-0.61	-0.46	0.38	0.42	1.73	1.10	1.00	33	16
OE-01, PI-01 *5	-0.39	-0.22	-0.55	-0.36	0.29	0.37	1.76	0.31	1.00	30	17

Reaction (4)	Olig-biotite zone				Upper staurolite zone						
Samples	Ga	Ch	Pa	Ms	St	Bi	Pl	Qz	H_2O		
OP-08, YA-01	-0.45	-0.07	-0.28	-0.39	0.27	0.33	0.94	0.59	1.00	20	26

Reaction (5)	Olig-biotite zone			Upper staurolite zone					
Samples	Zo	Pa	Qz	As	Ms	Pl	H_2O		
OP-08, YA-01	-0.19	-0.50	-1.00	0.81	0.05	1.28	1.00	22	24

Enami
Table 4.

Table 5. Data used in calculation of dP/dT.

Solids

	V (cm^3/mole)		V (cm^3/mole)
Garnet (2)	118 *1	Zoisite	136 *1
(3) (4)	117 *1	Paragonite	264 *1
Biotite	301 *2	Muscovite (2) (3) (4)	282 *2
Hornblende	273 *3	(5)	281 *1
Chlorite	423 *4	Sillmanite	49.9 *1
Glaucophane	264 *2	Plagioclase	100 *1
Omphacite	63 *5	Quartz	22.7 *1
Staurolite	223 *2		

H_2O

	V (cm^3/mole)	$\Delta S_{dehyd.}$ (cal/deg mole)
P = 7 Kb T = 600 °C	20.5 *6	12.5 *7
P = 10 Kb T = 600 °C	18.6 *6	11.5 *7

Appendix

Table 1. Mineral assemblages of epidote amphibolites and basic and pelitic schists.

Sample	Rock type	Ga	Bi	Hb	Ch	Pa	Ms	Cz	Zo	Pl	Mc	Qz	Sp	Ru	Po	Py	Cp	Cm
OB-01	Bs		+	+	+		+	+		+		+		+	+		+	
AE-01	Ea	+		+	+	+	+	+		+		+	+	+				
AP-01	Ps	+					+	+		+	+	+				+		+
OE-01	Ea	+		+		+	+	+		+		+	+	+		+		
OE-02	Ea	+		+			+	+	+	+		+	+	+	+			

Enami
Appendix Table 1.

Appendix Table 2.

Chemical compositions of major constituent minerals.

Sample	OB-01			AE-01			
Mineral	Bi	Hb	Ch	Ga	Hb	Ch	Pa
SiO_2	39.4	45.6	28.4	37.9	46.8	26.9	46.5
TiO_2	1.22	0.46			0.28		0.11
Al_2O_3	18.0	14.8	18.9	21.6	10.9	21.3	39.4
FeO*	11.0	10.7	18.1	26.5	13.8	17.4	0.75
MnO	0.08	0.18	0.31	1.46	0.22	0.21	0.00
MgO	16.9	12.2	21.8	4.50	12.5	21.1	0.12
CaO	0.03	10.4	0.00	8.35	9.59	0.03	0.22
Na_2O	0.16	2.35			3.57		7.20
K_2O	8.38	0.37			0.26		0.68
Total	95.1_7	97.0_6	87.5_1	100.3_1	97.9_2	86.9_4	94.9_8
Si	5.687	6.597	5.759	2.972	6.833	5.472	5.974
Al^{IV}	2.313	1.403	2.241	0.028	1.167	2.528	2.026
Al^{VI}	0.748	1.120	2.275	1.968	0.708	2.578	3.938
Ti	0.132	0.050			0.031		0.011
Fe^{2+*}	1.327	1.294	3.069	1.737	1.685	2.959	0.081
Mn	0.010	0.022	0.053	0.097	0.027	0.036	0.000
Mg	3.634	2.629	6.585	0.526	2.719	6.394	0.023
Ca	0.005	1.611	0.000	0.701	1.500	0.007	0.030
Na	0.045	0.659			1.010		1.792
K	1.542	0.068			0.048		0.111

Appendix Table 2.

Chemical compositions of major constituent minerals (continued).

Sample	AP-01		OE-01			
Mineral	Ga	Mc	Ga	Hb	Pa	Ms
SiO_2	38.2	65.8	38.7	42.8	47.1	51.4
TiO_2		0.00		0.46	0.18	0.25
Al_2O_3	20.6	18.8	21.3	16.6	38.9	28.8
FeO*	14.9	0.00	26.9	14.0	0.95	2.62
MnO	3.54	0.00	2.52	0.21	0.00	0.00
MgO	0.15	0.00	4.83	10.1	0.15	2.69
CaO	22.4	0.00	6.26	10.4	0.35	0.06
Na_2O		0.28		2.98	6.62	1.04
K_2O		15.8		0.42	1.10	8.43
Total	99.7_9	100.6_8	100.5_1	97.9_7	95.3_5	95.2_9
Si	3.006	3.005	3.024	6.276	6.034	6.782
Al^{IV}		1.012		1.724	1.966	1.218
Al^{VI}	1.910		1.961	1.144	3.906	3.260
Ti		0.000		0.051	0.017	0.025
Fe^{2+*}	0.980	0.000	1.757	1.716	0.102	0.289
Mn	0.236	0.000	0.167	0.026	0.000	0.000
Mg	0.018	0.000	0.562	2.206	0.029	0.529
Ca	1.888	0.000	0.524	1.633	0.048	0.008
Na		0.025		0.847	1.643	0.266
K		0.920		0.079	0.180	1.418